JOURNAL OF MATERIALS SCIENCE 30 (1995) 5192–5198

Cyclic fatigue of a sintered Al_2O_3/ZrO_2 ceramic

KAI DUAN*, YIU WING MAI
Centre for Advanced Materials Technology, Department of Mechanical and Mechatronic Engineering, The University of Sydney, NSW 2006, Australia

B. COTTERELL
Department of Mechanical and Production Engineering, National University of Singapore, Singapore 0511

A systematic experimental and theoretical study on the crack growth behaviour of a sintered Al_2O_3/ZrO_2 ceramic under cyclic loading is presented. It is found that in the cyclic fatigue experiments conducted on the single-edge-notched beam (SENB) geometry, for similar testing conditions, the crack growth rates are significantly faster than those under static fatigue. Al_2O_3/ZrO_2 therefore suffers genuine mechanical fatigue. Further experiments with the compact tension (CT) geometry show that the mechanical fatigue effect arises mainly from the degradation of the bridging mechanism. A theoretical analysis based on the compliance technique and a power law relationship between the crack-wake bridging stress and the crack-face separation is developed to evaluate quantitatively the degradation of the bridging stress due to cyclic fatigue.

1. Introduction

Al_2O_3/ZrO_2 ceramics exhibit much higher fracture toughness than traditional ceramics because of the addition of the zirconia (ZrO_2) phase. The improved crack tolerance mainly results from the microstructural changes induced by the transformation of tetragonal ZrO_2 to monoclinic ZrO_2 during both loading and fabrication upon cooling. This represents a new class of ceramics known as "zirconia toughened alumina" (ZTA). The major transformation-related toughening mechanisms include microcracking and transformation toughening, either separately or conjointly [1–4]. Experimental studies have also revealed other toughening mechanisms which are not directly related to the transformation of t-ZrO_2 to m-ZrO_2. For example, it is found that the enhanced thermal shock resistance in a sintered Al_2O_3/ZrO_2 is a consequence of the microcracking mechanism, which is caused by the interaction of the polycrystalline dispersed phase and the severe anisotropy of thermal expansion of the monoclinic zirconia [5, 6], and that the increased fracture resistance is mainly caused by crack-wake bridging [7–9].

As a result of these crack toughening mechanisms, Al_2O_3/ZrO_2 ceramics usually exhibit a R-curve characteristic, i.e. the fracture resistance (R) increases with crack growth. The effects of the R-curve are known to have improved the mechanical reliability of ceramic materials by increasing the Weibull modulus [10–13] and enhanced the resistance to environmental-assisted slow crack growth [7–14]. Consequently, the lifetimes of ceramic components are significantly improved [7, 15].

However, it has been reported that the same crack toughening mechanisms which give rise to the R-curve behaviour can be considerably degraded when subjected to cyclic loading, i.e. the toughened materials suffer genuine mechanical fatigue [16–24]. Many studies on zirconia-containing ceramics reached this conclusion because the crack growth rates under cyclic stresses were substantially larger than those under static stresses of the same magnitude. However, the mechanisms for the increased crack growth rates were not well understood though plasticity-related mechanisms were suggested by Davidson *et al.* [25] who observed the formation of slip bands like in metal fatigue and by Liu and Chen [22, 23] who found the damage accumulation as revealed by the hysteresis loop of the stress–plastic strain curve for several partially stabilized zirconia ceramics.

In a recent paper Mai *et al.* [15] have suggested that mechanical fatigue in zirconia-based ceramics can be caused by a reduction of the intrinsic fracture toughness and/or a degradation of the crack-wake toughening mechanisms so that crack shielding is decreased. For the Mg–PSZ ceramics Hoffman *et al.* [26] have shown that mechanical fatigue is a direct consequence of the decrease of the intrinsic toughness due to the rupture of the tetragonal precipitates in the crack tip region. In the present study an example is given on

* *Present address*: CSIRO Division of Exploration and Mining, PO Box 883, Kenmore, Qld 4069, Australia

0022–2461

a ZTA ceramic for which the major mechanism for cyclic fatigue is the degradation of the crack bridges developed behind the crack tip. Experiments are first conducted to demonstrate the mechanical fatigue effect on crack growth and then a theoretical analysis is performed to evaluate the reduction of crack bridging stress with cyclic loading.

2. Material and experiments

The ZTA ceramic was made in the CSIRO Division of Materials Science and Technology. The alumina powder with 8 wt % ZrO_2 and 0.3 wt % PVA mixed according to the procedures given by Garvie *et al.* [6] was formed in the dies of various sizes and shapes with ~ 10 MPa and isopressed with 120 MPa. The green bodies formed were then sintered at 1600 °C for 1 h in air. The theoretical density of the samples after sintering was $\sim 96\%$. All the specimens were ground and polished to 1 μm to facilitate observations of the microstructure and crack growth.

The microstructures of the sintered Al_2O_3/ZrO_2 ceramic were examined by using a 35C scanning electron microscope (SEM) on a polished, thermally etched and carbon coated surface. Fig. 1 reveals that the monoclinic ZrO_2 particles exist in the form of agglomerates and are embedded in the Al_2O_3 matrix. As a result of the coarse agglomerates, the microcrack density and size in the material were enhanced. Observations of the polished surface also confirmed the existence of flaws. The microcracks in the material were mainly located along the grain boundaries and in the vicinity of the transformed ZrO_2 particles during cooling. This ZTA ceramic material has been shown to possess very good thermal shock resistance and is most suitable for use as an advanced refractory [6].

In an earlier study [9] it has been demonstrated that the material exhibits a pronounced *R*-curve behaviour and a nonlinear stress–strain curve due to crack bridging and microcracking [8, 9]. Fig. 2 shows the *R*-curves measured in several specimen geometries including double-cantilever-beam (DCB), compact tension (CT) and single-edge-notched beam (SENB). Because of the large scale bridging in the crack wake region the *R*-curves show dependence on both specimen geometry and size [27, 28]. *In-situ* crack growth observation and microscopic studies have also confirmed the presence of a crack wake bridging zone. Because of the pronounced *R*-curve in this ZTA material, it is expected to suffer mechanical fatigue.

The cyclic fatigue experiments were conducted on two sizes of the SENB, $\sim 3.5 \times 6 \times 35$ mm^3 (referred to as small SENB) and $\sim 5.5 \times 11.5 \times 80$ mm^3 (referred to as large SENB) and CT geometries. The stress intensity factor (SIF) and crack-mouth-opening-displacement (CMOD) expressions used in analysing the experimental data for these two types of specimens can be easily found in the literature. Cyclic loads with sinusoidal waveform were used for all the specimens and crack growth was monitored with an optical microscope by periodically removing the specimen from the fatigue testing machine.

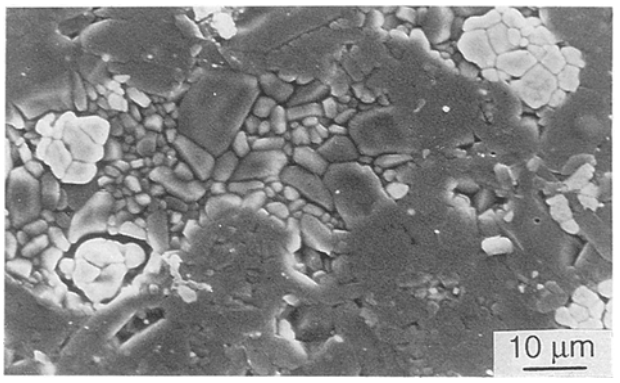

Figure 1 The microstructure of a sintered Al_2O_3/ZrO_2 composite. This SEM photograph was taken on a thermal-etched polished surface.

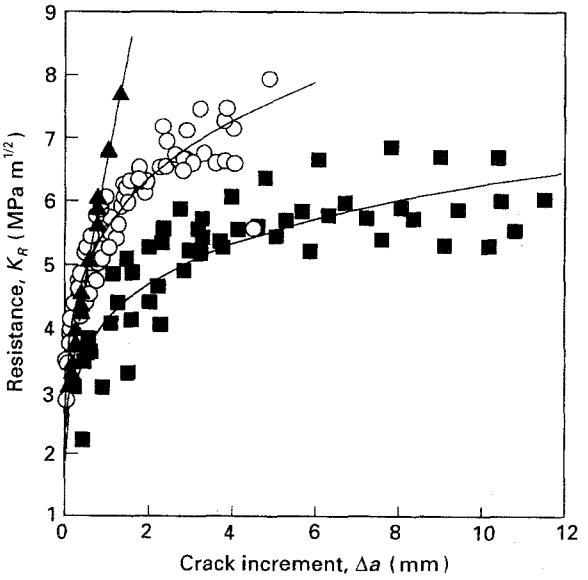

Figure 2 Crack-resistance curves for the ZTA ceramic showing the effects of specimen geometry and size. ■ DCB; ○ CT; ▲ SENB.

The small SENB's were loaded in a piezoelectric bimorph actuator system via four-point bending with 5/30 mm inner/outer spans. The frequency used was 180 Hz, the load ratio ($\sigma_{min}/\sigma_{max}$) was fixed at 0.1 and the relative humidity was $50 \sim 60\%$. The large SENBs were tested with a sinusoidal stress at 20 Hz in an Instron 8501 fatigue testing machine in four-point bending with 20/40 mm inner/outer spans. Several stress ratios, 0.1, 0.3, 0.5 and 0.9, were used and the experiments were completed with a controlled temperature, $22 \sim 23$ °C.

To identify the degradation mechanism due to cyclic stress, environmental-assisted slow crack growth experiments were performed with small SENB specimens in a static loading device under a Ziess optical microscope. The loading system consisted of a square frame with a threaded bar which drove a four-point bending fixture producing a deflection on the specimen [8, 9]. The strains were measured by four strain gauges attached on the frame and converted into a force using a calibration curve. The SIF can be

calculated based on the force and crack length so that a V–K curve may be plotted.

The CT specimen was first applied a monotonic load so that a crack growth of approximately 4 mm was produced and the bridging stresses built up. Then this specimen was subjected to a sinusoidal load at 20 Hz and a stress ratio of 0.1. The maximum load was chosen so that no further crack growth could occur under cyclic loading. The fatigue test was periodically interrupted and the compliance was measured by reloading to a maximum load less than that used in cyclic fatigue.

3. Observed crack growth behaviour under cyclic loading

3.1. Existence of genuine mechanical fatigue mechanism

With small SENB specimens, the slow crack growth rates under both static and cyclic loading conditions have been measured and the results are plotted in Fig. 3 against the maximum stress intensity factor K_{max}. It can be seen that the crack growth rate subjected to static loading was negligible if the applied stress intensity factor K_a was less than a critical value ~ 9 MPa m$^{1/2}$, which could be considered as the threshold stress intensity factor for environmental-assisted slow crack growth. However, under cyclic loading, the threshold value is much lower than that for static loading. Also, high crack growth rates could be measured in cyclic loading at maximum stress intensity factors lower than the static loading threshold. These results all indicate the existence of a genuine mechanical fatigue effect in this ZTA ceramic.

In ceramic materials toughened by crack-wake bridging such as coarse-grained alumina mechanical fatigue is caused by the degradation of the bridges which reduces the closure stress with the elapsed cycles [29–31]. This effect can be confirmed by observing the compliance changes as the bridges are being progressively damaged. For the ZTA studied here the bridge degradation mechanism was verified by the following tests on a CT specimen. Firstly, a monotonic load was exerted on the specimen to produce a crack extension of about 4 mm and establish crack bridging as shown by the K_R-curve in Fig. 4(a). Subsequently, a cyclic load with the maximum less than that required for further crack extension was applied and the changes in compliance CMOD/P were plotted against elapsed cycles N in Fig. 4(b). It is seen that the measured compliance values increase gradually with elapsed cycles N, which indicates that the bridging stress built up during the monotonic loading has been significantly degraded by the cyclic stress. This experiment has further confirmed the existence of a true mechanical fatigue in the ZTA ceramic.

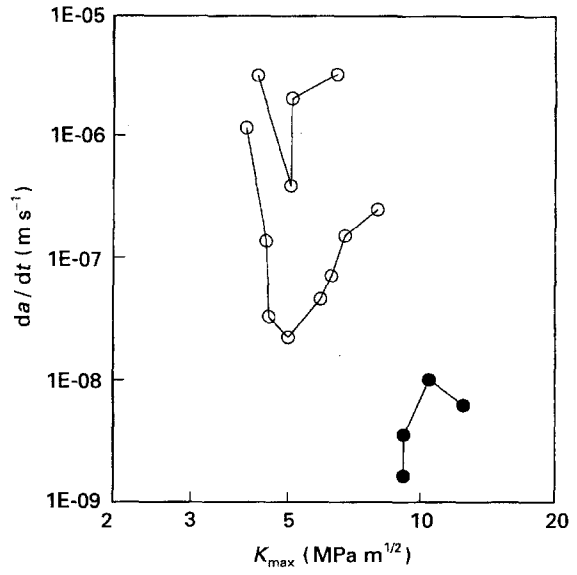

Figure 3 Crack growth of SENB ZTA specimen under cyclic (○) and static (●) loading conditions.

3.2. Crack growth rates under cyclic loading

The crack growth rates, da/dN, under cyclic loading is often expressed as a power law function of the stress intensity factor range, ΔK, because of the dominant role of ΔK in controlling the crack growth. However, other factors such as load ratio $\sigma_{min}/\sigma_{max}$ and the

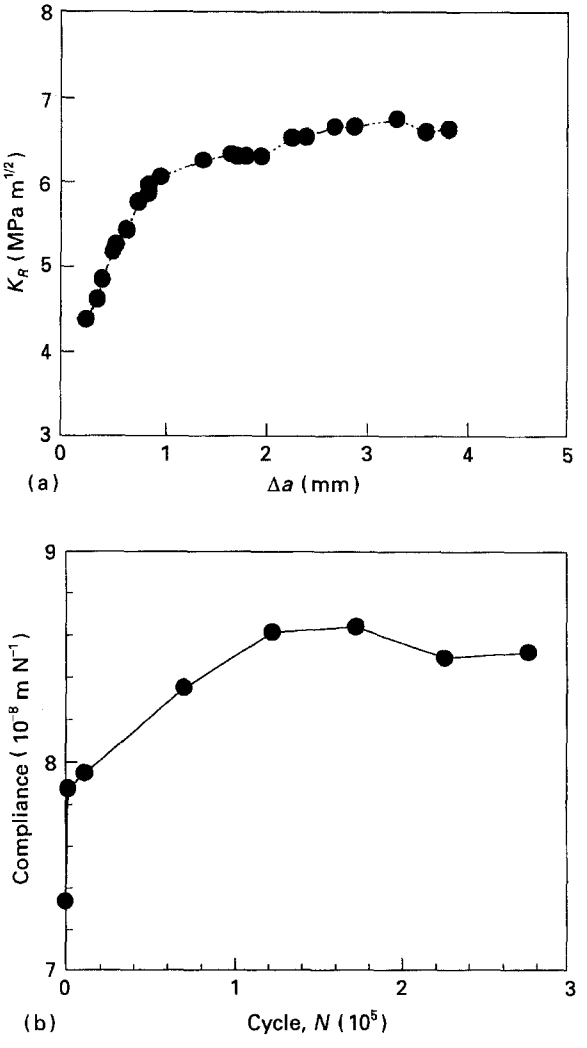

Figure 4 The results of a monotonic-cyclic loading test on a CT specimen: (a) K_R-curve obtained in monotonic loading; and (b) the compliance change during cyclic loading (with no crack growth) indicating the degradation of the crack wake bridges.

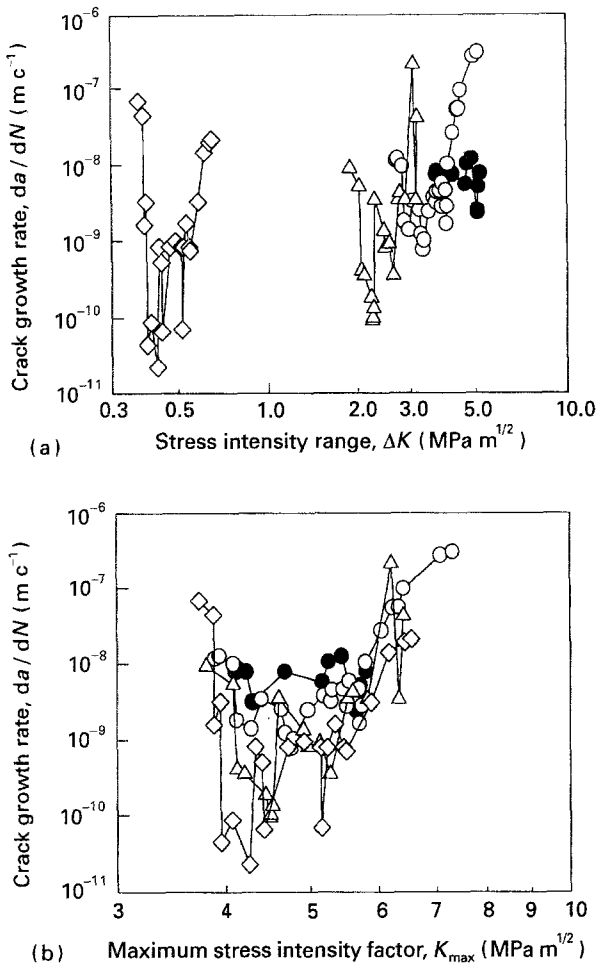

Figure 5 Cyclic crack growth rates, da/dN of large SENB ZTA specimens with different stress ratio plotted against (a) stress intensity factor range, ΔK, and (b) maximum stress intensity factor, K_{max}. ● R = 0.1; ○ R = 0.3; △ R = 0.5; ◇ R = 0.9.

maximum stress intensity factor K_{max}, etc. can significantly affect the crack growth. As a result, considerable effort has been spent to investigate these effects on fatigue crack growth.

In this study, large SENBs have been subjected to cyclic loads with several fixed load ratios, K_{min}/K_{max} = 0.1, 0.3, 0.5 and 0.9. The measured da/dN data are given in Fig. 5 where it is seen that the crack growth curves shift towards the left with increasing load ratio when plotted against the stress intensity factor range ΔK (Fig. 5(a)) and almost fall within the same range against the maximum stress intensity factor K_{max} (Fig. 5(b)), i.e. the crack growth rates are mainly controlled by K_{max} rather than ΔK. The strong dependence of cyclic crack growth on K_{max} has also been reported in other zirconia-bearing ceramics [17, 22, 23] and was fitted by an empirical equation which is written as [17]

$$\mathrm{d}a/\mathrm{d}N = A_c(K_{Ic}^0/K_{Ic})^m[\Delta K/(1-R)]^m = A_c(K_{Ic}^0/K_{Ic})^m K_{max}^m \quad (1)$$

where K_{Ic}^0 and K_{Ic} are respectively the toughness of the materials without and with toughening and R is the stress ratio. For a given material, the K_{Ic}^0/K_{Ic} ratio is a constant and the above equation can be simplified to

$$\mathrm{d}a/\mathrm{d}N = BK_{max}^m = B[\Delta K/(1-R)]^m \quad (2)$$

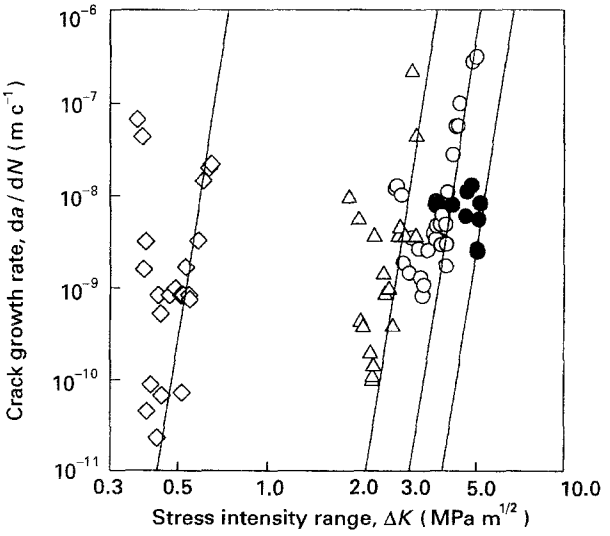

Figure 6 Comparisons of da/dN–ΔK data with predictions from Equation 2 for different stress ratios. ● R = 0.1; ○ R = 0.3; △ R = 0.5; ◇ R = 0.9; —— predicted.

By fitting the data on the rising portion of the da/dN–K_{max} curves in Fig. 5(b) to Equation 2, the values of B and m can be calculated through a regression procedure. The da/dN–ΔK lines for different load ratios estimated from these B and m values are plotted in Fig. 6 and there is reasonable agreement with the experimental data. Careful scrutiny of the experimental data in Fig. 5(b) shows the crack growth rates to decrease slightly with increasing R. This has also been observed by Liu and Chen [22, 23] on cyclic fatigue of an yttria–stabilized zirconia. This weak dependence of cyclic fatigue crack growth on the load ratio implies that da/dN can be empirically expressed as [22, 23]

$$\mathrm{d}a/\mathrm{d}N = C\Delta K^2 K_{max}^{m-2} \quad (3)$$

Note that neither Equation 2 nor 3 can describe the data for R = 1.0 which is the static fatigue case. It should be noted in Fig. 5 that the cyclic crack growth takes place in a discontinuous fashion which has not been understood well. Equation 2 was only used to give the best fit to the cyclic fatigue data obtained.

3.3. Effects of *R*-curves behaviour on cyclic crack growth

It has been emphasized previously [15] that true mechanical fatigue often results from the R-curve behaviour and our experiments found that the R-curves have significantly affected the whole crack growth process. A specific feature of the da/dN–K_{max} curves shown in Figs 3 and 5 is that the crack growth rates initially decrease with increasing K_{max} and then after a certain amount of crack growth, rise again. This descending–ascending characteristic is similar to that observed for environmental–assisted slow crack growth in other ZrO_2 ceramics which is caused by the R-curve mechanisms operating during crack extension [14].

In a similar way the R-curve changes the crack growth rate in a cyclically located ceramic component

through its effect on the crack tip stress intensity factor K_t. The crack growth usually starts at a higher speed when $K_t = K_a$ because there is no toughening. The subsequent resistance increase with crack extension makes K_t apparently less than K_a. Two situations can occur with the crack growth. Initially, the resistance increment ΔK_R due to the crack toughening can be larger than the increase in the K_a due to the increased crack length. Consequently, the macrocrack growth rate decreases with crack extension. When the crack extension resistance is close to the plateau value, the increment in K_a due to crack growth overtakes the shielding term ΔK_R and the crack growth rate da/dN increases with the advancing crack. Hence the cyclic fatigue crack growth behaviour is as obtained in Fig. 5.

4. Estimation of bridging stress degradation

4.1. Theoretical basis

It has been shown in Section 3 that mechanical fatigue in the ZTA ceramic is caused by the degradation of the crack-wake bridging mechanism under cyclic loading. This damage effect can be modelled by the reduction of crack closure stress with increasing elapsed cycles using the compliance technique developed by Hu and Mai [30, 31].

Let $C(a)$ be the compliance of a specimen with a crack length a without bridging and $C_u(x)$ the compliance measured in an experiment for the same a but with a bridging zone x. It is expected that

$$C(a) \geqslant C_u(x) \tag{4}$$

The function $C_u(x)$ represents the compliance with an unsaturated bridging zone developed during crack extension or that with a bridging zone which has been fully developed and then partially removed by sawcutting [30]. The changes in compliance with crack extension can be related to the bridging stress $\sigma_b(x)$ at a distance x from the crack tip by [29, 30]

$$\frac{\sigma_b(x)}{\sigma_m} = \frac{C^2(a)}{C'(a)}\frac{C'_u}{C_u^2} \tag{5}$$

where σ_m is the maximum bridging stress. Usually, the bridging stress $\sigma_b(x)$ is a function of the crack opening displacement $w(x)$. For ligament and grain bridging in ceramic materials the σ_b–w relation generally obeys a strain–softening law approximated by [32]

$$\sigma_b = \sigma_m\left[1 - \frac{w}{w_c}\right]^n \tag{6}$$

where w_c is the critical crack opening displacement at which point the bridging stress is zero. Once this relationship is determined the theoretical crack–resistance (K_R) curve can be predicted based on procedures described earlier [32]. However, an iterative technique is needed to determine σ_m and n to give the best fit to the R-curve data.

For most ceramic materials, a further assumption for simplification can be made in that the crack surfaces remain straight as the crack propagates. Consequently, the above strain–softening equation can be rewritten as

$$\sigma_b = \sigma_m\left[1 - \frac{x}{X}\right]^n \tag{7}$$

where X is the maximum bridging zone size. Substituting Equation 7 in to 5 and integrating both sides leads to a ϕ-function

$$\phi = [C(a)/C'(a)][C(a)/C_u - 1] = \begin{cases} X/(n+1) & \Delta a \geqslant X \\ [X/(n+1)][1 - (1 - \Delta a/X)] & \Delta a < X \end{cases} \tag{8}$$

This $\phi(\Delta a)$ function allows the n value and the saturated bridging zone X to be determined easily from the experimental compliance data. When the K_R data are given, the maximum bridging stress σ_m can be determined so that the whole bridging stress function is obtained [8, 9].

When a specimen containing a crack of length a with a saturated bridge zone X developed in a steady-state crack propagation test is subjected to a given cyclic stress such that no further crack extension can be produced, the changes in ϕ-function with elapsed cycles N can be written as [29, 30].

$$\phi(N) = [C(a)/C'(a)][C(a)/C_u(N) - 1] = X(N)/(n+1) \tag{9}$$

The above equation shows that the damage of bridging stress from cyclic loading is equivalent to a reduction of the bridging zone length $X(N)$. Let N_c be the critical number of fatigue cycles elapsed for the given cyclic loading system to destroy all existing bridges. If $N = N_c$, $X(N_c) = 0$ so that $C_u(N_c) = C(a)$ and $\phi(N_c) = 0$. The difference between the ϕ-functions for monotonic and cyclic loading can be written as

$$\Delta\phi = \phi(a) - \phi(N) = \begin{cases} [X - X(N)]/(n+1) & N < N_c \\ X/(n+1) & N \geqslant N_c \end{cases} \tag{10}$$

The length of bridging zone $X(N)$ during cyclic fatigue test can be determined by the changes in ϕ value, i.e.

$$X(N) = (n+1) \times \phi(N) = X - (n+1) \times \Delta\phi(N) \tag{11}$$

4.2. Estimating the degradation of crack bridging stress due to cyclic loading

We recall that the pronounced K_R-curve behaviour of this ZTA material shown in Fig. 2 is mainly caused by crack wake bridging though microcracking may also contribute to the increase in crack resistance [8, 9]. Based on the ϕ-function theory [30, 31], the crack bridging stress parameters, σ_m and n, are estimated respectively at 91 MPa and 2.33.

Using the data in Fig. 4 and Equations 9 and 10, the $\phi(N)$ and $\Delta\phi(N)$ values of the CT specimen subjected to $K_{max} = 3.16\ \mathrm{MPa\,m^{1/2}}$, $R = 0.1$ and 20 Hz were estimated as shown in Fig. 7. It can be seen that

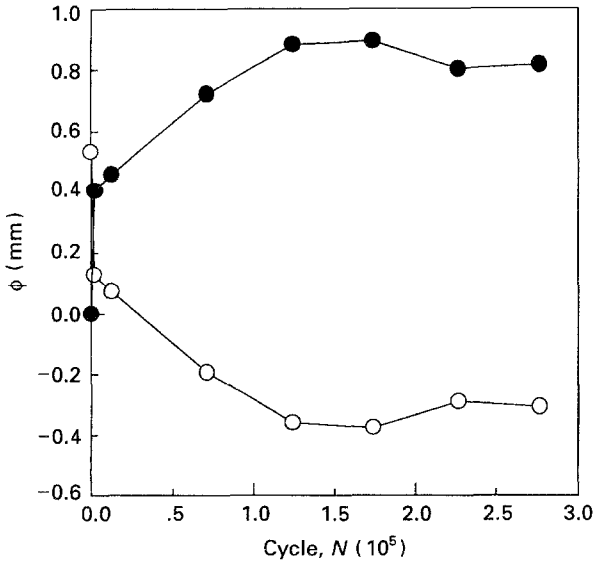

Figure 7 ϕ (○) and $\Delta\phi$ (●) functions with elapsed cycles in a CT ZTA specimen when the crack length is kept constant.

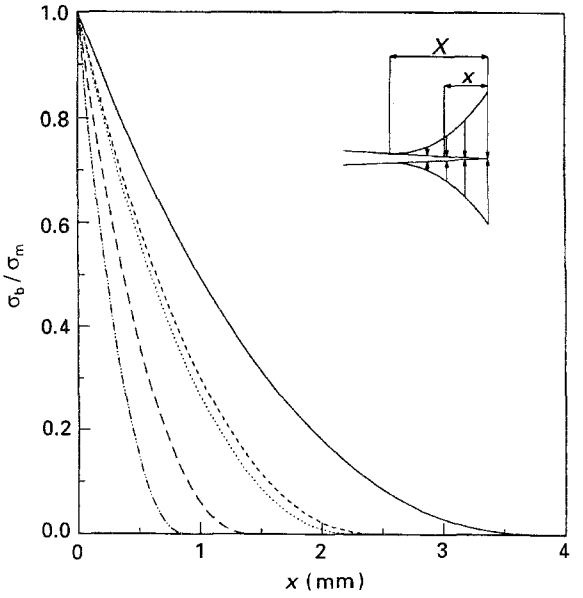

Figure 8 The change of bridging stress with elapsed cycles in a CT ZTA specimen when the crack length is kept constant. (K_{max} = 3.16 MPa m$^{1/2}$, R = 0.1 and frequency = 20 Hz.) N values, — 0; – – – – 2000; - - - - - 12000; – – – – 71000; – . – . – . > 124000.

ϕ decreases rapidly in the beginning with elapsed cycles and then remains at a relatively steady value. This indicates that after N_c cycles, no further damage of the crack bridges can be produced by the cyclic loading. After all the bridges are destroyed, the ϕ-function assumes a negative value which reflects the effect of the microcrack damage zone around the crack tip [30, 31].

From Fig. 4, it is found that in the CT specimen, the saturated bridging zone (X) was reached at a crack extension of 3.84 mm. Therefore, substituting X = 3.84 mm and n = 2.33 in Equation 11, the variation of the bridging zone size $X(N)$ with elapsed cycle N becomes

$$X(N) = 3.84 - 3.33\,\Delta\phi(N) \quad (12)$$

Using Equation 12 and the data in Fig. 7 together with the bridging stress equation (Equation 7), we obtain the dependence of the bridging stress with elapsed cycles N as shown in Fig. 8. It is obvious that the bridging zone size decreases with cycle N if the functional form of the bridging stress and the maximum bridging stress σ_m remain unchanged.

The degradation of the bridging stress manifested by the decreasing bridging zone size may contribute to cyclic fatigue crack growth in two ways. Firstly, the reduction of crack shielding due to cyclic loading leads to an increase in the crack tip stress intensity factor so that slow crack growth due to environmental corrosion is enhanced. Secondly, when the crack resistance K_R is degraded too much so that it is less than the applied stress intensity factor K_a, a crack increment must be created to maintain mechanical equilibrium. Consequently, the measured crack growth rate in cyclic loading is larger than that in static loading.

5. Conclusions

Both experimental and theoretical studies have shown the existence of a genuine mechanical fatigue effect in a ZTA ceramic for advanced refractory applications. Experiments with SENB specimens showed that the crack growth rates in cyclic loading were faster than those in a statically loaded specimen and had a much lower cyclic fatigue threshold. It was also confirmed by the observation that the measured compliances CMOD/P of a CT specimen with a crack extension produced by prior monotonic loading increased with elapsed cycles N. Since no crack extension was produced by the cyclic loading the increase in compliance must come from the degradation of the crack bridges in the wake region.

Further cyclic loading tests of SENB specimens over a range of load ratios from 0.1 to 0.9 showed that the cyclic crack growth of this ZTA ceramic was mainly dependent on the maximum stress intensity factor K_{max} and slightly on the stress intensity factor range ΔK. The R-curve behaviour obviously played an important role in the whole cyclic crack growth process. Thus, the measured da/dN–K_{max} curves exhibit a descending–ascending characteristic and crack growth was intermittent rather than continuous. The ϕ-function technique by Hu and Mai [30, 31] has been successfully used to analyse and predict the degradation of the bridging stress due to mechanical fatigue.

Acknowledgements

We wish to thank the Australian Research Council for the support of this work. Useful discussions with X.-Z. Hu, S. Lathabai, T. Liu, and M.V. Swain are much appreciated.

References

1. N. CLAUSSEN, J. STEEB and R. F. PABST, *Bull. Am. Ceram. Soc.* **56** (1977) 559.
2. A. G. EVANS and R. M. CANNON, *Acta Metall.* **34** (1986) 761.

3. M. RÜHLE, *Mater. Sic. Engng* **A105/106** (1988) 77.
4. J. WANG and R. STEVENS, *J. Mater. Sci.* **24** (1989) 3421.
5. R. C. GARVIE and M. F. GOSS, in "Advanced ceramics II", edited by S. Sõmiya (Elsevier, London, 1988) p. 69.
6. R. C. GARVIE, M. F. GOSS, S. MARSHALL and C. URBANI, *Mater. Sci. Forum* **34–36** (1988) 681.
7. M. V. SWAIN, *Mater. Forum* **9** (1986) 34.
8. K. DUAN, Ph.D. Thesis, The University of Sydney, Sydney (1993).
9. K. DUAN, Y.-W. MAI and B. COTTERELL, in Proceedings of the twenty-fifth National Symposium on Fracture Mechanics, Bethlehem, PA, June/July 1993 (ASTM special publications, STP 1220) in press.
10. K. KENDALL, N. McN. ALFORD and J. D. BIRCHALL, in Materials Research Society Symposia Proceedings, Vol. 78, Advanced Structural Ceramics, edited by P. F. Becher, M. V. Swain and S. Sõmiya, (Materials Research Society, Pittsburgh, PA, 1987), p. 189.
11. K. KENDALL, N. McN. ALFORD, S. R. TAN and J. D. BIRCHALL, *J. Mater. Res.* **1** (1986) 120.
12. K. DUAN, Y.-W. MAI and B. COTTERELL, *Key Engineering Materials*, **48–50** (1990) 53.
13. *Idem., J. Mater. Sci.* **30** (1995) 1405.
14. K. DUAN, B. COTTERELL and Y.-W. MAI, in Fracture Mechancis: 23rd Symposium, ASTM STP 1189, edited by R. Chona (ASTM, Philadelphia, 1993) p. 788.
15. Y.-W. MAI, X.-Z. HU, K. DUAN and B. COTTERELL, in "Fracture mechanics of ceramics", 9, edited by R. C. Bradt, D. P. H. Hasselman, D. Munz, M. Sakai and V. Ya. Shevchenko (Plenum Press, New York, 1992) p. 387.
16. R. H. DAUSKARDT, W. C. CARTER, D. K. VEIRS and R. O. RITCHIE, *Acta Metall. et Mater.* **38** (1990) 2327.
17. R. H. DAUSKARDT, D. B. MARSHALL and R. O. RITCHIE, *J. Amer. Ceram. Soc.* **73** (1990) 893.
18. R. H. DAUSKARDT, W. YU and R. O. RITCHIE, *J. Amer. Ceram. Soc.* **70** (1987) C248.
19. L. A. SYLVA and S. SURESH, *J. Mater. Sci.* **24** (1989) 1729.
20. C. J. BEEVERS, D. C. CARDONA and P. BOWEN, *J. Hard Mater* **2** (1991) 207.
21. J.-F. TSAI, C.-S. YU and D. K. SHETTY, *J. Amer. Ceram. Soc.* **73** (1990) 2992.
22. S.-Y. LIU and I.-W. CHEN, *Ibid.* **74** (1991) 1197.
23. *Idem., J. Amer. Ceram. Soc.* **74** (1991) 1206.
24. F. GUIU, M. J. REECE and D. A. J. VAUGHAN, *J. Mater. Sci.* **26** (1991) 3275.
25. D. L. DAVIDSON, J. B. CAMPBELL and J. LANKFORD, *Acta Metall. et Mater.* **39** (1990) 1319.
26. M. J. HOFFMAN, S. WAKAYAMA, Y.-W. MAI, M. KAWAHARA and T. KISHI, *J. Amer. Ceram. Soc.* in press.
27. B. COTTERELL and Y.-W. MAI, *Mater. Forum* **11** (1988) 341.
28. *Idem., J. Mater. Sci.* **22** (1987) 2734.
29. S. LATHABAI, J. RÖDEL and B. R. LAWN, *J. Amer. Ceram. Soc.* **74** (1991) 1340.
30. X.-Z. HU and Y.-W. MAI, *J. Mater. Sci.* **27** (1992) 3502.
31. *Idem., J. Amer Ceram. Soc.* **75** (1992) 848.
32. R. M. L. FOOTE, Y.-W. MAI and B. COTTERELL, *J. Mech. Phys. Solids* **34** (1986) 593.

Received 26 August
and accepted 10 October 1994